NTSE-2013 Keynote Talk:

Nuclear Forces from Lattice Quantum Chromodynamics

Martin J. Savage

Institute for Nuclear Theory, Box 351550, Seattle, WA 98195-1550, USA

Abstract

A century of coherent experimental and theoretical investigations have uncovered the laws of nature that underly nuclear physics. The standard model of strong and electroweak interactions, with its modest number of input parameters, dictates the dynamics of the quarks and gluons — the underlying building blocks of protons, neutrons, and nuclei. While the analytic techniques of quantum field theory have played a key role in understanding the dynamics of matter in high energy processes, they encounter difficulties when applied to low-energy nuclear structure and reactions, and dense systems. Expected increases in computational resources into the exa-scale during the next decade will provide the ability to numerically compute a range of important strong interaction processes directly from QCD with quantifiable uncertainties using the technique of lattice QCD. These calculations will refine the chiral nuclear forces that are used as input into nuclear many-body calculations, including the three- and four-nucleon interactions. I discuss the state-of-the-art lattice QCD calculations of quantities of interest in nuclear physics, progress that is expected in the near future, and the impact upon nuclear physics.

Keywords: *Nuclear forces; lattice QCD*

1 Introduction

A nucleus is at the heart of every atom, and loosely speaking, is a collection of protons and neutrons that interact pairwise, with much smaller, but significant, three-body interactions. We are fortunate to know that the underlying laws governing the strong interactions result from a quantum field theory called quantum chromodynamics (QCD). It is constructed in terms of quark and gluon fields with interactions determined by a local SU(3) gauge-symmetry and, along with quantum electrodynamics (QED), underpins all of nuclear physics when the five relevant input parameters, the scale of strong interactions $\Lambda_{\rm QCD}$, the three light-quark masses m_u, m_d and m_s, and the electromagnetic coupling α_e, are set to their values in nature. It is remarkable that the complexity of nuclei emerges from "simple" gauge theories with just five input parameters. Perhaps even more remarkable is that nuclei resemble collections of nucleons and not collections of quarks and gluons. By solving QCD, we are expecting to predict, with arbitrary precision, nuclear processes and the properties of multi-baryon systems.

The fine-tunings observed in the structure of nuclei, and in the interactions between nucleons, are peculiar and fascinating aspects of nuclear physics. For the values

Proceedings of International Conference 'Nuclear Theory in the Supercomputing Era — 2013' (NTSE-2013), Ames, IA, USA, May 13–17, 2013. Eds. A. M. Shirokov and A. I. Mazur. Pacific National University, Khabarovsk, Russia, 2014, p. 156.

http://www.ntse-2013.khb.ru/Proc/Savage.pdf.

of the input parameters that we have in our universe, the nucleon-nucleon (NN) interactions are fine-tuned to produce unnaturally large scattering lengths in both s-wave channels [described by non-trivial fixed-points in the low-energy effective field theory (EFT)], and the energy levels in the ^{8}Be-system, ^{12}C and ^{16}O are in "just-so" locations to produce enough ^{12}C to support life, and the subsequent emergence and evolution of the human species. At a fundamental level it is important for us to determine the sensitivity of the abundance of ^{12}C to the light-quark masses and to ascertain the degree of their fine-tuning.

Being able to solve QCD for the lightest nuclei, using the numerical technique of lattice QCD (LQCD), would allow for a partial unification of nuclear physics. It would be possible to "match" the traditional nuclear physics techniques — the solution of the quantum many-body problem for neutrons and protons using techniques such as No-Core Shell Model (NCSM), Green's Function Monte Carlo (GFMC), and others, to make predictions for the structure and interactions of nuclei for larger systems than can be directly calculated with LQCD. By placing these calculations on a fundamental footing, reliable predictions with quantifiable uncertainties can then be made for larger systems.

2 Chiral nuclear forces

During the 1990's, the nuclear forces were systematized by the hierarchy emerging from the spontaneously broken chiral symmetries of QCD. The resulting small expansion parameters are powers of the external momenta and powers of the light-quark masses normalized to the scale of chiral symmetry breaking, as pioneered by Weinberg, first in the meson sector and then the multi-nucleon sector [1–3]. In addition to generating nuclear forces that are consistent with QCD, this construction provides the calculational advantage of parametric estimates of the systematic uncertainty introduced by the truncation of the nuclear interactions at a given order in the expansion. The actual ordering of contributions remains a subject of debate even today, with Weinberg's chiral expansion of the potential having its peculiar difficulties, as does the KSW expansion of scattering amplitudes [4, 5]. Calculations are being performed at a sufficiently high order where the size of truncation errors is quite small. Weinberg's ordering of operators based upon a chiral expansion of the n-body potentials between nucleons has been carried out to N^{3}LO, which includes contributions to the three-body (starting at N^{2}LO) and the leading four-body interactions (starting at N^{3}LO) (for a recent review see Ref. [6]).

During the last several years, nuclear structure calculations have been performed with the chiral nuclear forces, leading to both postdictions and predictions for nuclei to a given order in the expansion, and compared with experiment, e. g., see Fig. 1. The nuclear forces that are presently used in such calculations are constrained by experimental measurements of NN scattering and light nuclei. As the desired precision increases, which requires working to higher orders in the expansion, the number of required experimental constraints increases. Eventually, there are too few experimental constraints to practically reduce the systematic uncertainty below some level in any given calculation. However, LQCD calculations are expected to provide a way to constrain the nuclear forces beyond what is possible with experiment, and hence to further reduce the systematic uncertainties in nuclear structure calculations. Beyond providing direct calculations of important quantities, LQCD calculations of the light nuclei and nuclear forces can

1. verify experimental constraints and/or reduce the uncertainties in the constraints imposed by experiment,

2. constrain components of the nuclear forces that are inaccessible to experiment,

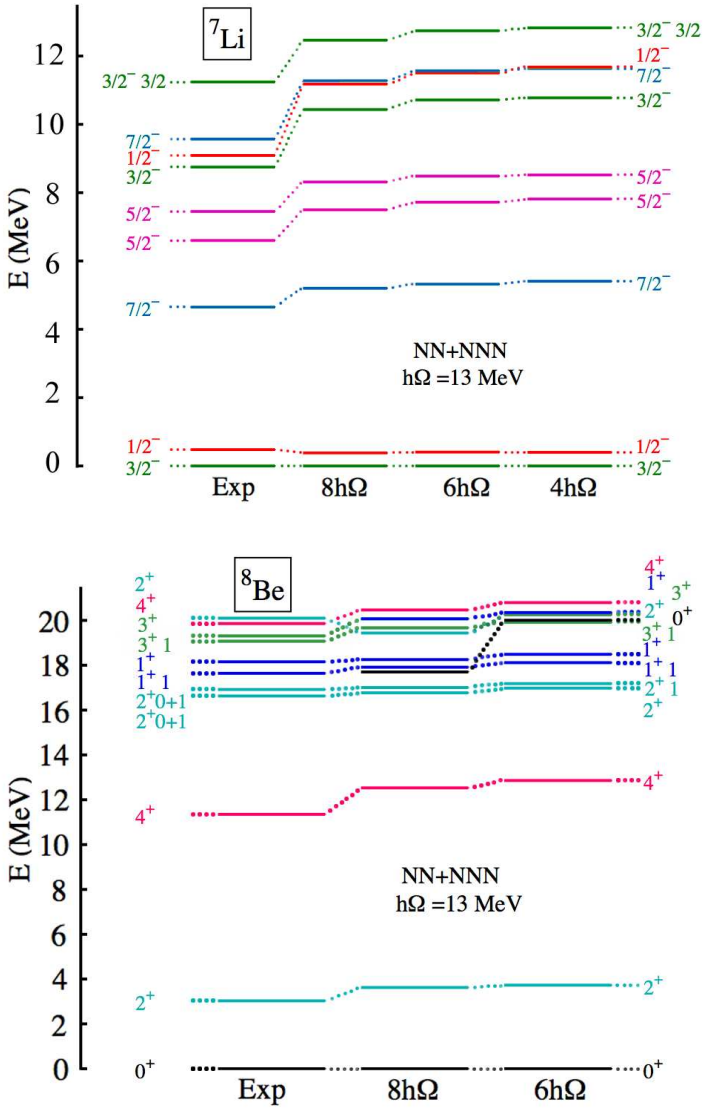

Figure 1: NCSM calculations of lowest-lying levels in ^{7}Li and ^{8}B using chiral nuclear forces [7]. Image is reproduced with the permission of P. Maris.

for instance the light-quark mass dependences which dictates some of the multi-pion vertices, and multi-neutron forces,

3. constrain counterterms at higher orders in the expansion to further reduce the systematic uncertainties.

3 Lattice QCD

LQCD is a technique in which space-time is discretized into a four-dimensional grid and the QCD path integral over the quark and gluon fields at each point in the grid is performed in Euclidean space-time using Monte Carlo methods. A LQCD calculation of a given quantity will deviate from its value in nature because of the finite volume of the space-time (with $L^3 \times T$ lattice points) over which the fields exist, and the finite separation between space-time points (the lattice spacing, b). However, such deviations can be systematically removed by performing calculations in multiple vol-

umes with multiple lattice spacings, and extrapolating using the theoretically known functional dependences on each. Supercomputers are needed for such calculations due to the number of space-time points and the Monte Carlo evaluation of the path integral over the dynamical fields. In order for a controlled continuum extrapolation, the lattice spacing must be small enough to resolve structures induced by the strong dynamics, encapsulated by $b\Lambda_\chi \ll 1$ where Λ_χ is the scale of chiral symmetry breaking. Further, in order to have the hadron masses, and also the scattering observables, exponentially close to their infinite-volume values, the lattice volume must be large enough to contain the lightest strongly interacting particle, encapsulated by $m_\pi L \gtrsim 2\pi$ where m_π is the mass of the pion and L is the extent of the spatial dimension of the cubic lattice volume (this, of course, can be generalized to non-cubic volumes). Effective field theory (EFT) descriptions of these observables exist for $b\Lambda_\chi \lesssim 1$ [the Symanzik action and its translation into chiral perturbation theory (χPT) and other frameworks] and $m_\pi L \gtrsim 2\pi$ (the p-regime of χPT and other frameworks). The low-energy constants in the appropriate EFT are fit to the results of the LQCD calculations, which are then used to take the limit $b \to 0$ and $L \to \infty$. Computational resources devoted to LQCD calculations are becoming sufficient to be able to perform calculations at the physical values of the light quark masses in large enough volumes and at small enough lattice spacings to be relevant, but the majority of present day calculations are performed with pion masses of $m_\pi \gtrsim 200$ MeV. Therefore, most calculations require the further extrapolation of $m_q \to m_q^{\rm phys}$, but do not yet include strong isospin breaking or electromagnetism. In principle, the gauge-field configurations that are generated in LQCD calculations can be used to calculate an enormous array of observables, spanning the range from particle to nuclear physics. In practice, this is becoming less common, largely due to the different scales relevant to particle physics and to nuclear physics. Calculations of quantities involving the pion with a mass of $m_\pi \sim 140$ MeV are substantially different from those of, say, the triton with a mass of $M(^3\mathrm{H}) \sim 3$ GeV, and with the typical scale of nuclear excitations being $\Delta E \sim 1$ MeV. Present day dynamical LQCD calculations of nuclear physics quantities are performed with $m_\pi \sim 400$ MeV, lattice spacings of $b \sim 0.1$ fm and volumes with spatial extent of $L \sim 4$ fm.

LQCD calculations are approached in the same way that experimental efforts use detectors to measure one or more quantities — the computer is equivalent to the accelerator and the algorithms, software stack, and parameters of the LQCD calculation(s) are the equivalent of the detector. The parameters, such as lattice spacing, quark masses and volume, are selected based upon available computational resources, and simulations of the precision of the calculation(s) required to impact the physical quantity of interest, i. e. simulations of the LQCD Monte Carlos are performed. The size of the computational resources required for cutting edge calculations are such that you only get "one shot at it". A typical work-flow of a LQCD calculation consists of three major components. The first component is the production of an ensemble of gauge-field configurations which contain statistically independent samplings of the gluon fields resulting from the LQCD action. The production of gauge-fields requires the largest partitions on the leadership class computational facilities, typically requiring $\gtrsim$ 128K compute cores. Present-day calculations have $n_f = 0$, 2, 2+1, 3, 2+1+1 dynamical light-quark flavors and use the Wilson, $\mathcal{O}(b)$-improved-Wilson, staggered (Kogut–Susskind), domain-wall or overlap discretizations, each of which have their own "features". It is the evaluation of the light-quark determinant (the determinant of a sparse matrix with dimensions $\gtrsim 10^8 \times 10^8$) that consumes the largest fraction of the resources. Roughly speaking, $\gtrsim 10^4$ Hybrid Monte Carlo (HMC) trajectories are required to produce an ensemble of 10^3 decorrelated gauge fields, but in many instances this is an under estimate. For observables involving quarks, a second component of production is the determination of the light-quark propagators on each of the configurations. The light-quark propagator from a given source point (an example of which

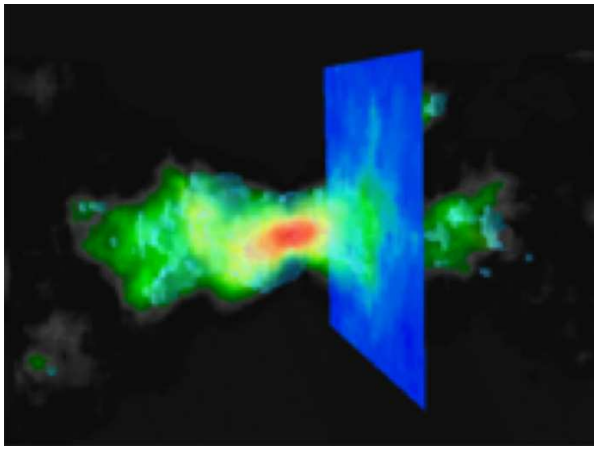

Figure 2: An example of (the real part of one component of) a light-quark propagator. The (blue) "wall" corresponds to the anti-periodic boundary conditions imposed in the time direction. Image is reproduced with the permission of R. Gupta.

is shown in Fig. 2) is determined by an iterative inversion of the quark two-point function, using the conjugate-gradient (CG) algorithm or variants thereof such as BiCGSTAB, or the most recently developed multi-grid (MG). During the last couple of years, the propagator production codes have been ported to run on GPU machines in parallel. GPU's can perform propagator calculations faster than standard CPU's by an order of magnitude, and have led to a major reduction in the statistical uncertainties in many calculations. There have been numerous algorithm developments that have also reduced the resources required for propagator production, such as the implementation of deflation techniques and the use of multi-grid methods. The third component of a LQCD calculation is the production of correlation functions from the light-quark propagators. This involves performing all of the Wick contractions that contribute to a given quantity. The number of contractions required for computing a single hadron correlation function is small. However, to acquire long plateaus in the effective mass plots (EMPs) that persist to short times, Lüscher–Wolff type methods involve the computation of a large number of correlation functions resulting from different interpolating operators, and the number of contractions can become large. In contrast, the naive number of contractions required for a nucleus quickly becomes astronomically large ($\sim 10^{1500}$ for uranium), but symmetries in the contractions, and new algorithms (e. g. Ref. [8]) greatly reduce the number of operations that must be performed. A further consequence of the hierarchy of mass scales is that there is an asymptotic signal-to-noise problem in nuclear correlation functions. The ratio of the mean value of the correlation function to the variance of the sample from which the mean is evaluated degrades exponentially at large times. However, this is absent at short and intermediate times and the exponential degradation of the signal-to-noise in the correlation functions can be avoided.

4 Cold nuclear physics with lattice QCD

Capability computing resources provided by leadership class computing facilities are used to produce ensembles of gauge-field configurations, while capacity computing resources, both those operated by USQCD and elsewhere are used to perform observable-dependent calculations of correlation functions using these configurations. Thus the capability resources enable a multitude of physics calculations to be accomplished with the capacity resources. In the area of cold nuclear physics there is currently a

well-defined set of goals, and a program in place to accomplish these goals, as described in one of the 2013 USQCD Whitepapers [9]: **Hadron Structure**, **Hadron Spectroscopy**, **Hadronic Interactions, Nuclear Forces and Nuclei**, and **Fundamental Symmetries**.

4.1 The spectra and structure of the hadrons

Before calculations of nuclei can be sensibly undertaken, the mass and structure of the nucleon must be reproduced in LQCD calculations. The spectrum of the lowest-lying hadrons calculated with LQCD is shown in Fig. 3, from which we observe that indeed LQCD is postdicting all of the light-hadron masses within uncertainties. Beyond its mass, one property of the nucleon that is well known experimentally is the forward-matrix element of the isovector axial current, g_A. Significant effort has been put into calculating g_A with LQCD, a summary of which is shown in Fig. 4, but the extrapolated LQCD value has consistently been smaller than the experimental value. With calculations beginning to be performed at the physical pion mass, the community is focused on understanding and quantifying the systematic uncertainties in these calculations.

A central element of the physics program at JLab is to determine the excited spectra of mesons and baryons, including searching for exotic states that are beyond the naive nonrelativistic quark model of hadrons, but arise naturally in QCD. A critical component of this program is the LQCD calculations of the spectra. They will play a central role in interpreting and understanding the experimental measurements. The spectra of such states is complicated by the presence of open multi-hadron channels and significant formal developments remain to be put in place before rigorous statements about the spectra can be made. Calculations at unphysical pion masses have been performed by the JLab LQCD group, examples of which are shown in Fig. 5, and remarkable progress has been made in the identification of states in these calculations. The aim is to have LQCD predict the exotic spectra of hadrons before, or at the same time as, the GlueX experiment at JLab runs, targeting the 2018 milestone HP15.

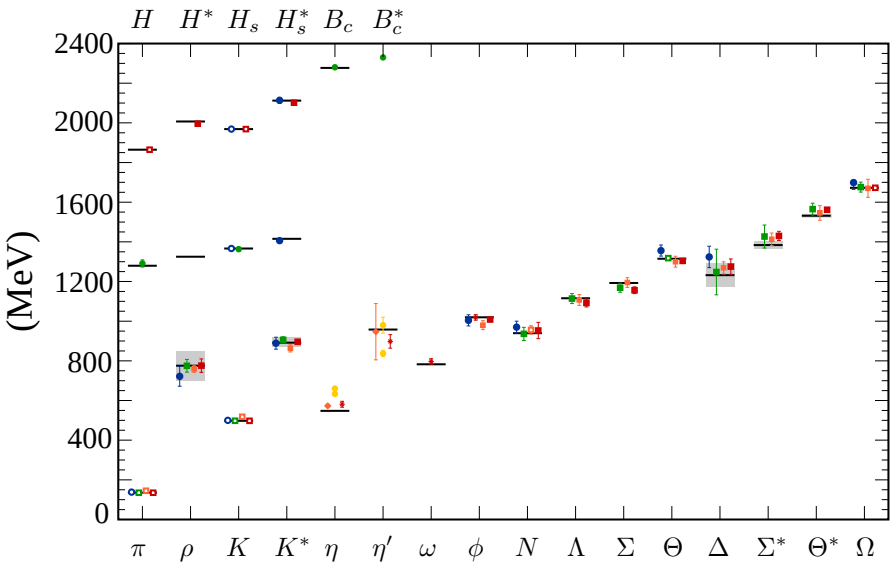

Figure 3: A summary of the low-lying hadron masses calculated with LQCD [10,11]. Image is reproduced with the permission of A. Kronfeld.

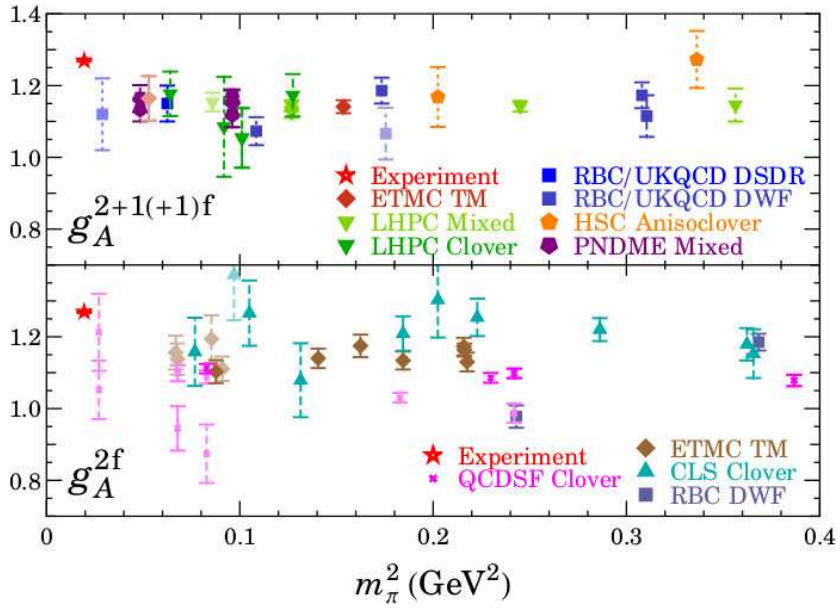

Figure 4: A summary of LQCD calculations of g_A [12]. Image is reproduced with the permission of H.-W. Lin.

4.2 Meson-meson scattering

Multi-hadron LQCD calculations are significantly more challenging than single-hadron calculations for a number of reasons, and systems involving baryons are even more challenging. Meson-meson systems are the simplest multi-hadron systems, and impressive progress has been made in the recent past, particularly when the LQCD calculations are combined with χPT. There is little or no signal-to-noise problem in such calculations and therefore highly accurate LQCD calculations of stretched-isospin states can be performed with modest computational resources. Moreover, the EFTs which describe the low-energy interactions of pions and kaons, including lattice-spacing and finite-volume effects, have been developed to non-trivial orders in the chiral expansion. The $I = 2$ pion-pion ($\pi^+\pi^+$) scattering length serves as a benchmark calculation with an accuracy that can only be aspired to in other systems. The scattering lengths for $\pi\pi$ scattering in the s-wave are uniquely predicted at LO in χPT [14]:

$$m_{\pi^+} a_{\pi\pi}^{I=0} = 0.1588, \quad m_{\pi^+} a_{\pi\pi}^{I=2} = -0.04537. \tag{1}$$

While experiments do not directly provide stringent constraints on the scattering lengths, a determination of s-wave $\pi\pi$ scattering lengths using the Roy equations has reached a remarkable level of precision [15, 16]:

$$m_{\pi^+} a_{\pi\pi}^{I=0} = 0.220 \pm 0.005, \quad m_{\pi^+} a_{\pi\pi}^{I=2} = -0.0444 \pm 0.0010. \tag{2}$$

The Roy equations [17] use dispersion theory to relate scattering data at high energies to the scattering amplitude near threshold. At present, LQCD can compute $\pi\pi$ scattering only in the $I = 2$ channel with precision as the $I = 0$ channel contains disconnected diagrams which require large computational resources. It is of great interest to compare the precise Roy equation predictions with LQCD calculations, and Fig. 6 summarizes theoretical and experimental constraints on the s-wave $\pi\pi$ scattering lengths [16]. This is clearly a strong-interaction process for which theory has somewhat out-paced the challenging experimental measurements.

Mixed-action $n_f = 2 + 1$ LQCD calculations, employing domain-wall valence quarks on a rooted staggered sea and combined with mixed-action χPT, have

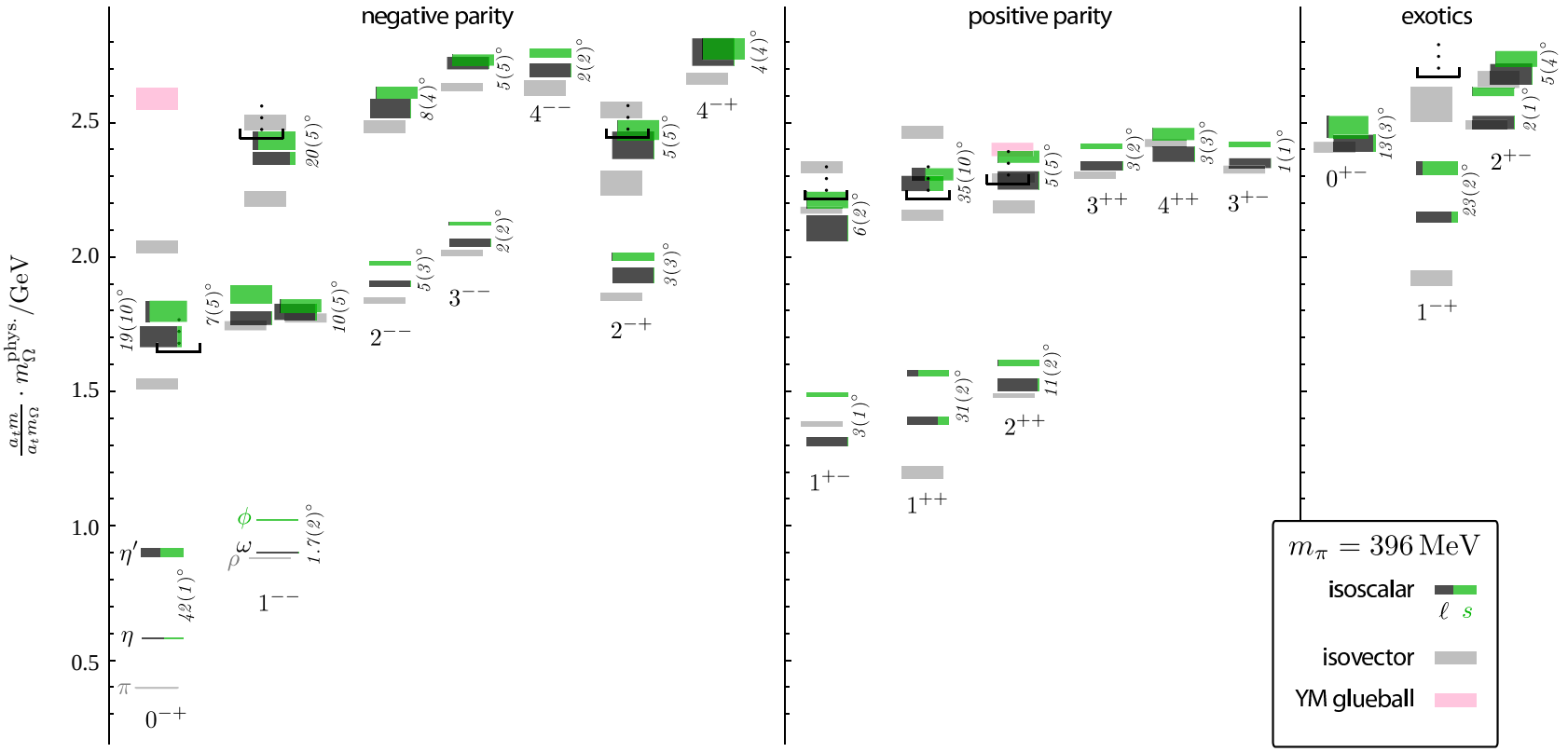

Figure 5: The spectra of isoscalar mesons calculated at $m_\pi \sim 396$ MeV by the JLab LQCD group [13] Image is reproduced with the permission of R. Edwards.

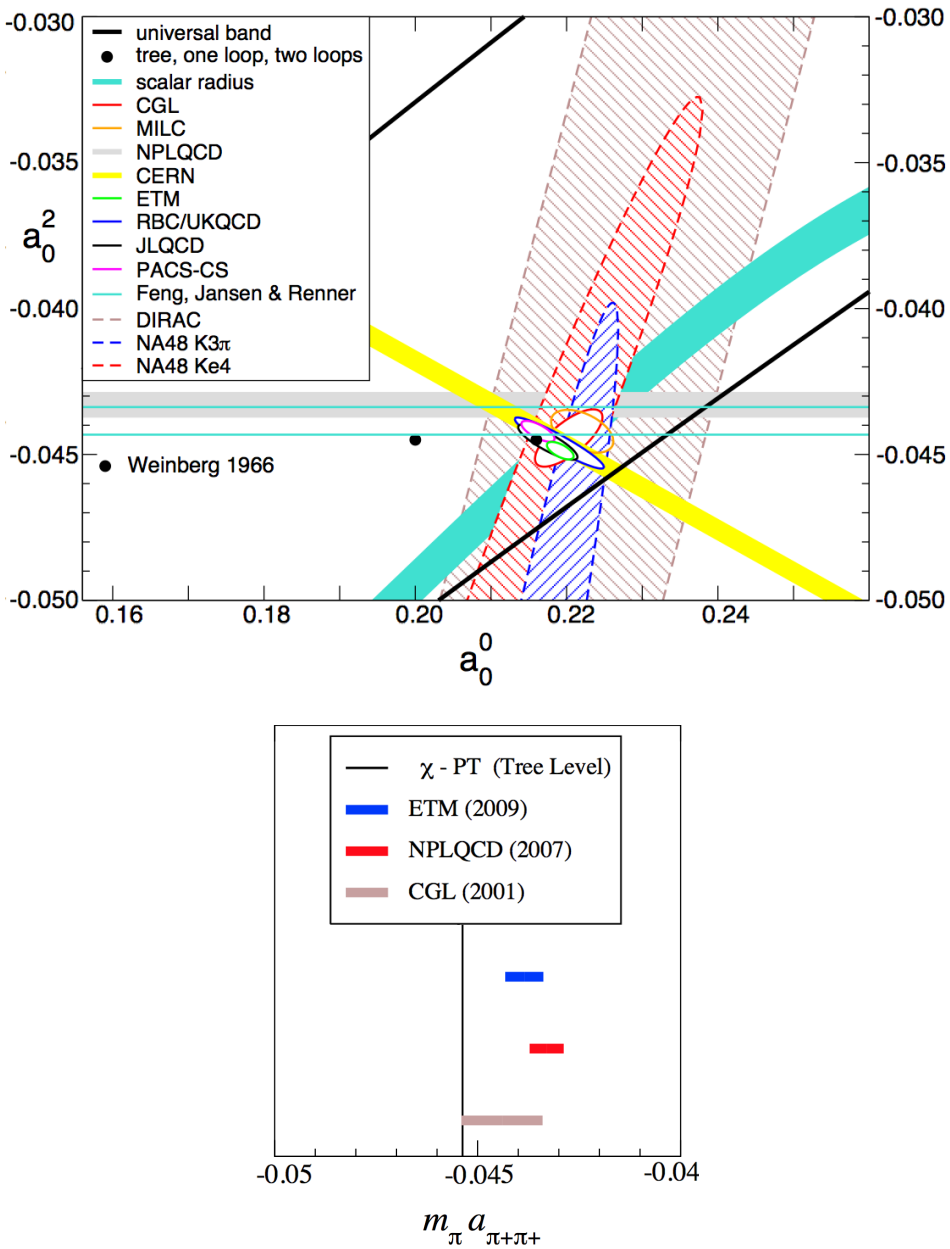

Figure 6: Constraints on threshold s-wave $\pi\pi$ scattering [16]. Image in the upper panel is reproduced with the permission of H. Leutwyler.

predicted [18]

$$m_{\pi^+} a_{\pi\pi}^{I=2} = -0.04330 \pm 0.00042 \tag{3}$$

at the physical pion mass. The agreement between this result and the Roy equation determination is a striking confirmation of the lattice methodology, and a powerful demonstration of the constraining power of chiral symmetry in the meson sector. However, LQCD calculations at one or more smaller lattice spacings, and with different discretizations, are required to verify and further refine this calculation. The ETM collaboration has performed a $n_f = 2$ calculation of the $I = 2$ $\pi\pi$ scattering length [19], producing a result extrapolated to the physical pion mass of

$$m_{\pi^+} a_{\pi\pi}^{I=2} = -0.04385 \pm 0.00028 \pm 0.00038. \tag{4}$$

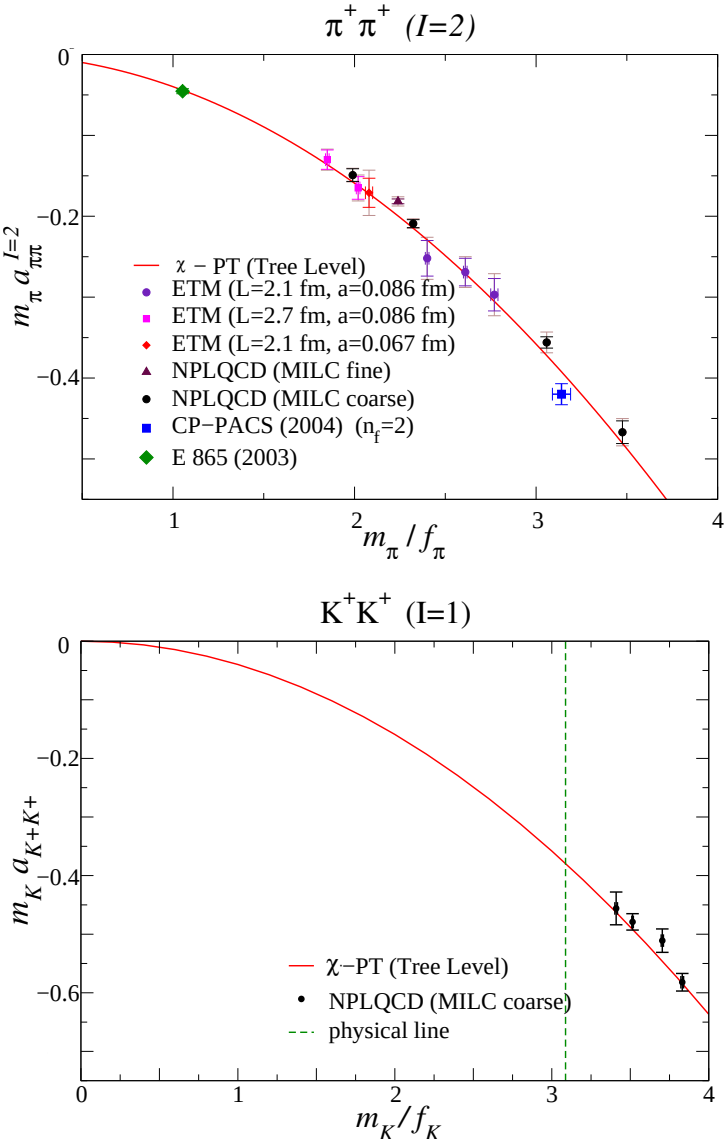

Figure 7: $m_{\pi^+}a_{\pi^+\pi^+}$ vs m_{π^+}/f_{π^+} (upper panel) and $m_{K^+}a_{K^+K^+}$ vs m_{K^+}/f_{K^+} (lower panel). The solid (red) curves are the current algebra predictions.

It is interesting to compare the pion mass dependence of the meson-meson scattering lengths to the current algebra predictions. In Fig. 7 (upper panel) one sees that the $I = 2$ $\pi\pi$ scattering length is consistent with the current algebra result up to pion masses that are expected to be at the edge of the chiral regime in the two-flavor sector. While in the two-flavor theory one expects fairly good convergence of the chiral expansion and, moreover, one expects that the effective expansion parameter is small in the channel with maximal isospin, the LQCD calculations clearly imply a degree of cancellation between chiral logs and counterterms. However, as one sees in Fig. 7 (lower panel), the same phenomenon occurs in K^+K^+ where the chiral expansion is governed by the strange quark mass and is therefore expected to be much more slowly converging. This remarkable conspiracy between chiral logs and counterterms for the meson-meson scattering lengths remains mysterious.

LQCD calculations of the meson-meson scattering phase-shifts are much less advanced than of the scattering length. This is because the calculation of the phase

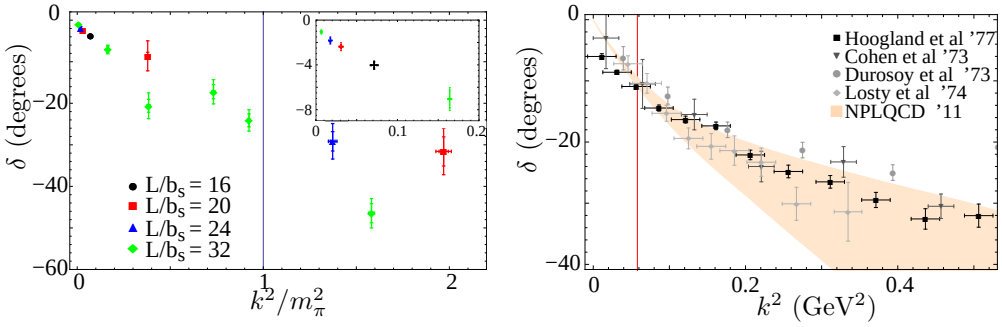

Figure 8: The $\pi^+\pi^+$ scattering phase-shift. The left panel shows the results of the LQCD calculations below the inelastic threshold ($|\mathbf{k}|^2 = 3m_\pi^2$) at a pion mass of $m_\pi \sim 390$ MeV [22]. The vertical (blue) line denotes the start of the t-channel cut. The shaded region in the right panel shows the results of the LQCD calculation extrapolated to the physical pion mass using NLO χPT, while the points and uncertainties corresponds to the existing experimental data. The vertical (red) line corresponds to the inelastic threshold.

shift, $\delta(E)$, at a given energy, E, requires a LQCD calculation of the two-meson correlation function at the energy E. Generally speaking, a given calculation can determine the lowest few two-hadron energy eigenvalues for a given momentum of the center-of-mass, and that multiple lattice volumes will allow for additional values of E at which to determine $\delta(E)$. The first serious calculation of the s-wave ($l = 0$) $I = 2$ $\pi\pi$ phase-shift was done by the CP-PACS collaboration with $n_f = 2$ at a relatively large pion mass [20], and more recently two groups have performed calculations at lower pion masses [21, 22], the results of which are shown in Fig. 8. Further, in some nice work by the Hadron Spectrum Collaboration (HSC), the first efforts have been made to extract the d-wave ($l = 2$) $I = 2$ $\pi\pi$ phase shift [21]. One of the more exciting recent results is the mapping out of the ρ-resonance at $m_\pi \sim 390$ MeV from the $\pi^+\pi^0$ energy-levels using Lüscher's method, as shown in Fig. 9 [23].

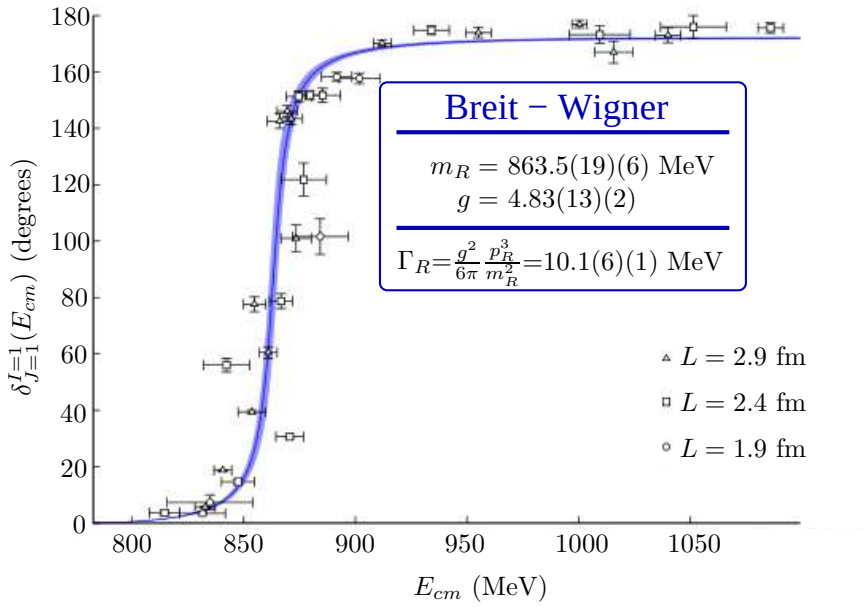

Figure 9: The ρ-resonance at a pion mass of $m_\pi \sim 390$ MeV [23]. Image is reproduced with the permission of R. Edwards.

4.3 Nuclear interactions

Calculations of the nucleon-nucleon scattering lengths have been successfully underway for the last decade [24–37] for a range of pion masses. Recently, LQCD calculations have been performed at $m_\pi \sim 800$ MeV that also provide the effective ranges [38], the results of which are shown in Fig. 10. Also shown are fits to the effective range expansion (ERE), including the shape parameter. The scattering length and effective range in the $^3S_1$ channel determined from the NLO fit to the ERE are

$$\begin{aligned} m_\pi a^{(^3S_1)} &= 7.45^{+0.57+0.71}_{-0.53-0.49}\,, & m_\pi r^{(^3S_1)} &= 3.71^{+0.28+0.28}_{-0.31-0.35}\,, \\ a^{(^3S_1)} &= 1.82^{+0.14+0.17}_{-0.13-0.12}\ \text{fm}, & r^{(^3S_1)} &= 0.906^{+0.068+0.068}_{-0.075-0.084}\ \text{fm}. \end{aligned} \tag{5}$$

The shape parameter obtained from the NNLO fit to the ERE expansion is: $Pm_\pi^3 = 2^{+5+5}_{-6-6}$. An interesting aspect of this result is that the ratio of scattering length to effective range, a measure of the naturalness of the system, is ∼2, which is to be compared with ∼3 at the physical quark masses. This leads one to speculate that

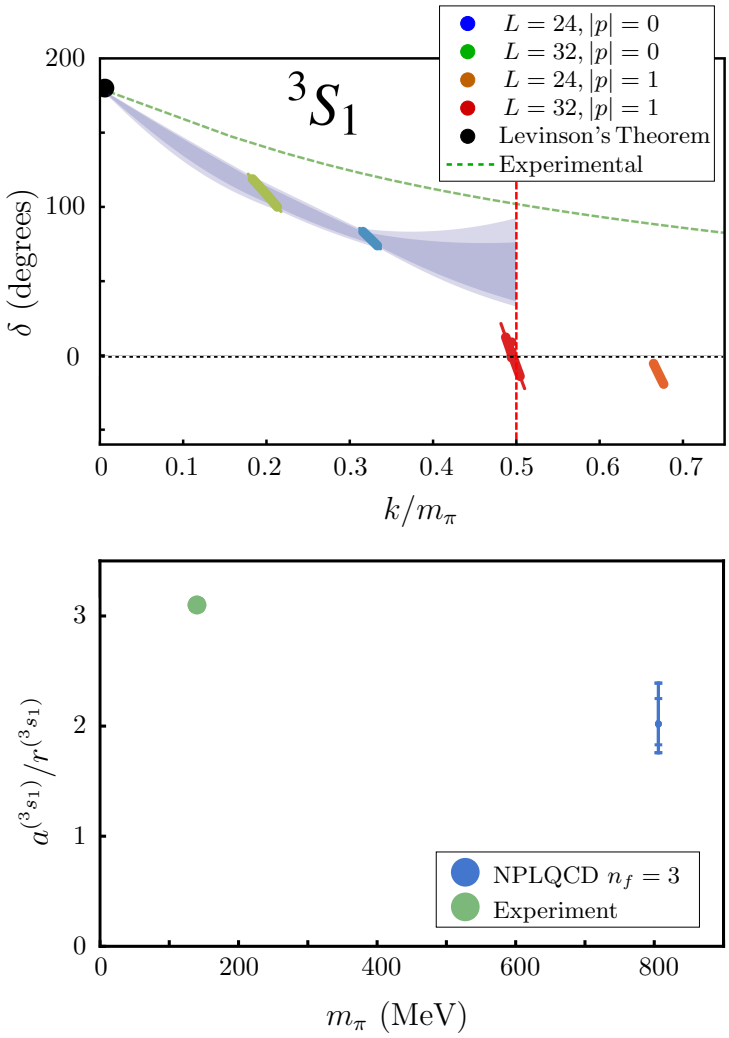

Figure 10: The upper panel shows the NN scattering phase shift in the $^3S_1$ channel extracted from LQCD calculations at the SU(3) symmetric point, including the fit to the ERE at N^{2}LO. The lower panel shows the ratio of the scattering length to effective range, a quantity that is a measure of the naturalness of the system.

the deuteron might be unnatural over a large range of quark masses and not just close to the physical values, indicating that it is not finely tuned. This speculation requires precise calculations at lighter quark masses to determine if this is, in fact, the situation.

4.4 Nuclei

Perhaps some of the most important LQCD calculations of late are those of the ground states of the light nuclei, including the deuteron, ^{3}He, ^{4}He and light hypernuclei. Fig. 11 shows the binding energy of the deuteron, ^{3}He and ^{4}He [34, 36, 37] as a function of the pion mass. Not only is it exciting to see nuclei emerge from QCD for a range of the light-quark masses, such calculations are crucial in dissecting and refining the chiral nuclear forces. However, it is clear that calculations at lighter pion masses are required, including at the physical pion mass. A summary of the energy-levels at the flavor SU(3) symmetry point found in the s-shell nuclei and hypernuclei [36] is shown in Fig. 12. These energy levels are elements of SU(3) irreps which allowed, in some cases, e. g., the H-dibaryon, the hypertriton and ${}^{\ \ 4}_{\Lambda\Lambda}$He, for distinct energy levels with the same spin and parity to be determined. Such calculations will become somewhat more complicated at lighter quark masses when the up and down quarks are not degenerate with the strange quark.

The calculations of NPLQCD and those of Yamazaki *et al.* are already shedding light on how the ground-state energies of the light nuclei approach their values at the physical light-quark masses. They are all bound at the heavier light-quark masses and become less bound as the quarks become lighter. In the case of the dineutron, which is bound at $m_\pi \sim 800$ MeV, it becomes unbound at some intermediate value of the pion mass, giving rise to a neutron-neutron system with an infinite scattering length.

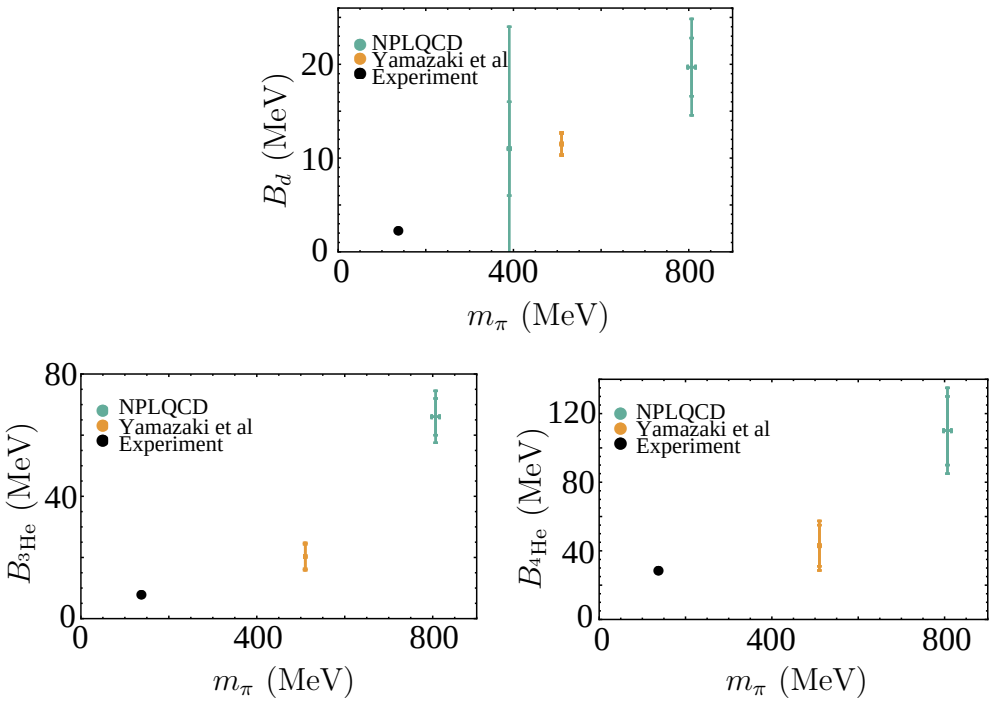

Figure 11: The deuteron (upper panel), ^{3}He (lower left panel) and ^{4}He (lower right panel) binding energies from $n_f = 2 + 1$ LQCD calculations [34, 36, 37].

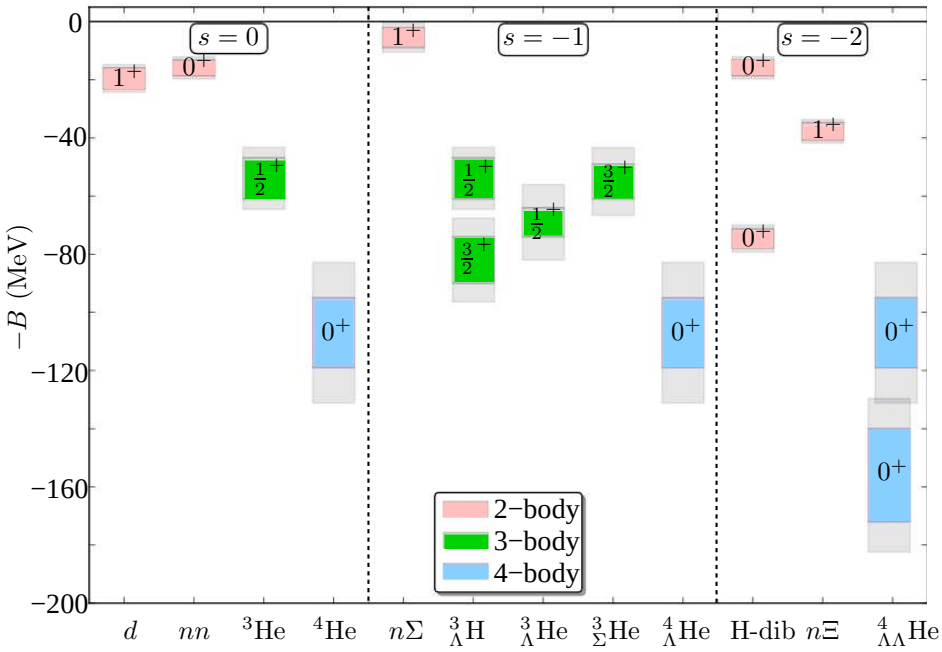

Figure 12: A compilation of the energy levels in light nuclei and hypernuclei in the limit of flavor SU(3) symmetry (with spin and parity J^π) calculated by NPLQCD [36] at a pion mass of $m_\pi \sim 800$ MeV.

One of the interesting aspects of the nuclear forces to explore is the tensor interaction, responsible for the mixing between the S-wave and D-wave channels in the deuteron channel. There is a series of LQCD calculations that can be performed that will permit an extraction of the SD mixing parameter, ϵ_1, using Lüscher's method [39–41], see Ref. [42].

4.4.1 Roadblocks of the past

It is important to understand how a few of the past roadblocks to progress in this area have been recently overcome. One of the roadblocks of the past was/is the "signal-to-noise problem" that afflicts states other than the pion. This problem is seen most simply in the single-nucleon correlation function, generated with a three-quark source and a three-quark sink. The variance of this correlation function is dictated by a 3-quark 3-anti-quark source and a 3-quark 3-anti-quark sink, which overlaps with both the $N\overline{N}$ and 3π intermediate states (and all others with the appropriate quantum numbers). At large times, the variance correlation function is dominated by the 3π intermediate state, while the single nucleon correlation function is dominated by the single nucleon, giving rise to an exponentially degrading signal. However, at intermediate times, the behavior of the "signal-to-noise" is determined by the overlap of the variance sinks and sources onto the intermediate hadronic states. The momentum projection onto single nucleon blocks, that NPLQCD is currently using, provides a volume suppression of the 3π intermediate state compared to the $N\overline{N}$ state. Thus, there is an intermediate time interval in which the signal-to-noise ratio is not exponentially degrading. It is in this time interval, dubbed the "Golden Window", that plateaus for the low-lying energy levels in light nuclei can be identified. Unfortunately, the window shrinks as the number of nucleons is increased, and so further developments will be required to go to much larger nuclei.

A second roadblock that inhibited progress in LQCD calculations of nuclei was the number of Wick contractions required to form a correlation function. A system con-

taining N_u up quarks and N_d down quarks requires $N_u!N_d!$ Wick contractions, which is a rapidly growing number as one moves beyond the nucleon. It was recognized that recursion relations relating the Wick contractions in systems with N mesons can be related to those with $N-1$ mesons [43]. Further, somewhat more sophisticated algorithms [8, 44] have been developed for the multi-baryon systems that greatly reduce the computing resources required to perform the contractions. These have led to very efficient calculations of the s-shell nuclei and hypernuclei, moving beyond the s-shell requires extensions of these works, and new ideas are required to calculate heavier nuclei.

4.5 The bridge between LQCD and nuclear structure

One of the points of discussion that came up during this presentation was how to optimally couple the results of LQCD calculations to nuclear structure calculations. Given the expertise in the nuclear structure community, it makes little sense for LQCD theorists to "go it alone" and attempt to calculate the entire periodic table. It makes much more sense for the LQCD theorists to produce sets of quantities that can be handed to the nuclear structure theorists who use them in their machinery to determine the periodic table. The question is what are the optimal quantities to pass along from LQCD.

It seems that the minimal set of quantities that could be passed along are the energy eigenvalues for a given system. LQCD calculations of the energy spectrum of an A-nucleon system could be performed in multiple lattice volumes, with multiple lattice spacings and at multiple light-quark masses, and handed to the the nuclear structure theorists who in turn reproduce the energies by tuning the chiral interactions. These tuned interactions are then used to calculate processes in the continuum. This methodology was used to calculate the $n\Sigma^-$ interactions at the physical pion mass using χPT [45]. The chiral interactions were tuned to reproduce the finite-volume energy levels determined in a series of LQCD calculations, and then used to calculate the scattering phase shift at the physical pion mass. Progress in this direction is starting to be made, as demonstrated in recent calculations by Nir Barnea and collaborators [46], by using the ground state energies of the deuteron, dineutron and ^{3}He at $m_\pi \sim 800$ MeV to reproduce the ^{4}He ground state using the pionless EFT.

5 Summary and final comments

I have summarized the rapid progress that is being made in developing LQCD into a reliable calculational tool for low-energy nuclear physics. It holds the promise to directly connect the structure and properties of nuclei with QCD, and to enable a refinement of the chiral nuclear forces that are used as input into nuclear structure calculations. At present, the ground states of the s-shell nuclei and hypernuclei are being calculated at unphysically heavy light-quark masses, but within the next few years, such calculations at $m_\pi \sim 140$ MeV will be performed (if hardware and software resources increase as expected). Within the next five years, the spectrum and interactions of the lightest nuclei and hypernuclei will be postdicted or predicted with fully-quantified uncertainties.

It is worth emphasizing that the LQCD effort in the US relies heavily on SciDAC funding to support the scientists who develop and optimize the software to run on the rapidly evolving computational hardware, e. g., GPU-accelerated compute nodes that comprise Titan at ORNL, or the BG/Qs at ANL and LLNL. Further, the effort requires ongoing access to both capability computing resources on leadership-class computing facilities, and capacity computing obtained from NERSC, XSEDE, through

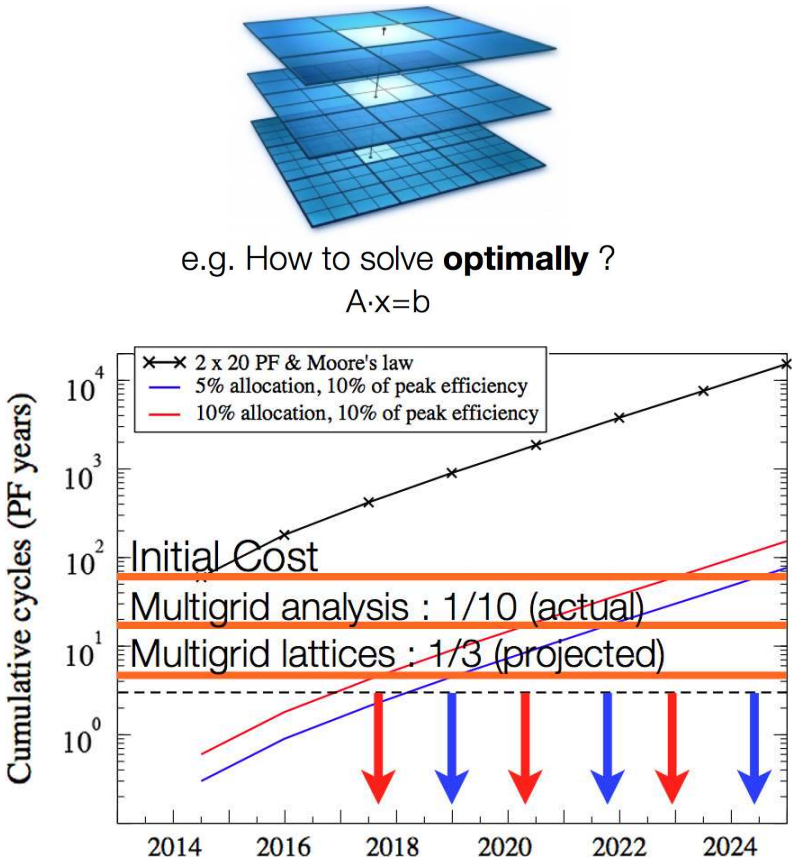

Figure 13: Multigrid is a recent algorithmic development to be implemented in LQCD calculations [47]. The horizontal (orange) cost estimates (that I have added to the original figure) provide one example of what is possible for a given production scenario. Parts of this image [48] are reproduced with the permission of B. Joo.

USQCD and at local compute clusters. Ongoing software (see Fig. 13) and hardware support are critical to progress in this area.

Ideally, one would start with a LQCD calculation and predict all of the quantities of interest in low-energy nuclear physics. Presently, we are not in a position to do this, even if significantly more computing resources were provided to the program. While Lüscher provided the formalism to relate the two-body S-matrix directly to two-particle energy levels inside a cubic volume with the fields subject to periodic boundary conditions [39, 40], which has since been understood and generalized to the two-nucleon systems, e. g. Ref. [41], such formalism is complicated to apply in coupled-channels systems [49–51]. Further, the formalism is not in place for the three- and higher-body sectors, but progress is being made in such systems [52, 53].

In closing, great progress is being made to reliably determine and refine the nuclear forces directly from QCD using lattice QCD.

Happy Birthday James: *James Vary is one of the first nuclear theorists I met when I arrived in the United States to enter the PhD program at Caltech in the mid 1980's. I recall James taking the time to talk physics with me during his stay. His detailed knowledge of, and passion for, important problems of the day left a lasting impression on me. Despite having been able to chat with, and even collaborate with, James since that time, when I learned that this conference was in part to celebrate James's 70th birthday, I was taken aback as it seems like yesterday that he was in his*

early 40's (and I was in my early 20's), and he has retained the same passion and energy for science. I should also add that James is responsible for me remembering the value of ħc! Happy 70$^{\text{th}}$*!!*

References

[1] S. Weinberg, Phys. Lett. B **251**, 288 (1990).

[2] S. Weinberg, Nucl. Phys. B **363**, 3 (1991).

[3] S. Weinberg, Phys. Lett. B **295**, 114 (1992), hep-ph/9209257 (1992).

[4] D. B. Kaplan, M. J. Savage and M. B. Wise, Phys. Lett. B **424**, 390 (1998), nucl-th/9801034 (1998).

[5] D. B. Kaplan, M. J. Savage and M. B. Wise, Nucl. Phys. B **534**, 329 (1998), nucl-th/9802075 (1998).

[6] E. Epelbaum and U.-G. Meissner, Ann. Rev. Nucl. Part. Sci. **62**, 159 (2012), arXiv:1201.2136 [nucl-th] (2012).

[7] P. Maris, J. P. Vary and P. Navrátil, Phys. Rev. C **87**, 014327 (2013), arXiv: 1205.5686 [nucl-th] (2012).

[8] W. Detmold and K. Orginos, Phys. Rev. D **87**, 114512 (2013), arXiv:1207.1452 [hep-lat] (2012).

[9] http://www.usqcd.org/collaboration.html#2013Whitepapers

[10] A. S. Kronfeld, Ann. Rev. Nucl. Part. Sci. **62**, 265 (2012), arXiv:1203.1204 [hep-lat] (2012).

[11] A. S. Kronfeld, arXiv:1209.3468 [physics.hist-ph] (2012).

[12] H.-W. Lin, PoS LATTICE 2012, 013 (2012), arXiv:1212.6849 [hep-lat] (2012).

[13] J. J. Dudek, R. G. Edwards, B. Joo, M. J. Peardon, D. G. Richards and C. E. Thomas, Phys. Rev. D **83**, 111502 (2011), arXiv:1102.4299 [hep-lat] (2011).

[14] S. Weinberg, Phys. Rev. Lett. **17**, 616 (1966).

[15] G. Colangelo, J. Gasser and H. Leutwyler, Nucl. Phys. B **603**, 125 (2001), hep-ph/0103088 (2001).

[16] H. Leutwyler, PoS CONFINEMENT8, 068 (2008), arXiv:0812.4165 [hep-ph] (2008).

[17] S. M. Roy, Phys. Lett. B **36**, 353 (1971).

[18] S. R. Beane, T. C. Luu, K. Orginos, A. Parreno, M. J. Savage, A. Torok and A. Walker-Loud, Phys. Rev. D **77**, 014505 (2008), arXiv:0706.3026 [hep-lat] (2007).

[19] X. Feng, K. Jansen and D. B. Renner, Phys. Lett. B **684**, 268 (2010), arXiv:0909.3255 [hep-lat] (2009).

[20] T. Yamazaki *et al.* (CP-PACS Collaboration), Phys. Rev. D **70**, 074513 (2004), hep-lat/0402025 (2004).

[21] J. J. Dudek, R. G. Edwards, M. J. Peardon, D. G. Richards and C. E. Thomas, Phys. Rev. D **83**, 071504 (2011), arXiv:1011.6352 [hep-ph] (2010).

[22] S. R. Beane *et al.* (NPLQCD Collaboration), arXiv:1107.5023 [hep-lat] (2011).

[23] J. J. Dudek, R. G. Edwards and C. E. Thomas, Phys. Rev. D **87**, 034505 (2013), arXiv:1212.0830 [hep-ph] (2012).

[24] M. Fukugita, Y. Kuramashi, H. Mino, M. Okawa and A. Ukawa, Phys. Rev. Lett. **73**, 2176 (1994), hep-lat/9407012 (1994).

[25] M. Fukugita, Y. Kuramashi, M. Okawa, H. Mino and A. Ukawa, Phys. Rev. D **52**, 3003 (1995), hep-lat/9501024 (1995).

[26] S. R. Beane, P. F. Bedaque, K. Orginos and M. J. Savage, Phys. Rev. Lett. **97**, 012001 (2006), hep-lat/0602010 (2006).

[27] S. R. Beane *et al.* (NPLQCD Collaboration), Phys. Rev. D **81**, 054505 (2010), arXiv:0912.4243 [hep-lat] (2009).

[28] N. Ishii, S. Aoki and T. Hatsuda, Phys. Rev. Lett. **99**, 022001 (2007), nucl-th/0611096 (2006).

[29] S. Aoki, T. Hatsuda and N. Ishii, Comput. Sci. Dis. **1**, 015009 (2008), arXiv: 0805.2462 [hep-ph] (2008).

[30] S. Aoki, T. Hatsuda and N. Ishii, Progr. Theor. Phys. **123**, 89 (2010), arXiv: 0909.5585 [hep-lat] (2009).

[31] T. Yamazaki, Y. Kuramashi and A. Ukawa, arXiv:1105.1418 [hep-lat] (2011).

[32] T. Yamazaki, Y. Kuramashi and A. Ukawa, Phys. Rev. D **81**, 111504 (2010), arXiv:0912.1383 [hep-lat] (2009).

[33] P. de Forcrand and M. Fromm, Phys. Rev. Lett. **104**, 112005 (2010), arXiv: 0907.1915 [hep-lat] (2009).

[34] S. R. Beane *et al.* (NPLQCD Collaboration), Phys. Rev. D **85**, 054511 (2012), arXiv:1109.2889 [hep-lat] (2011).

[35] T. Inoue *et al.* (HAL QCD Collaboration), Nucl. Phys. A **881**, 28 (2012), arXiv: 1112.5926 [hep-lat] (2011).

[36] S. R. Beane, E. Chang, S. D. Cohen, W. Detmold, H. W. Lin, T. C. Luu, K. Orginos, A. Parreno, M. J. Savage and A. Walker-Loud, arXiv:1206.5219 [hep-lat] (2012).

[37] T. Yamazaki, K. -I. Ishikawa, Y. Kuramashi and A. Ukawa, Phys. Rev. D **86**, 074514 (2012), arXiv:1207.4277 [hep-lat] (2012).

[38] S. R. Beane, E. Chang, S. D. Cohen, W. Detmold, P. Junnarkar, H. W. Lin, T. C. Luu, K. Orginos, A. Parreno, M. J. Savage and A. Walker-Loud, Phys. Rev. C **88**, 024003 (2013), arXiv:1301.5790 [hep-lat] (2013).

[39] M. Lüscher, Commun. Math. Phys. **105**, 153 (1986).

[40] M. Lüscher, Nucl. Phys. B **354**, 531 (1991).

[41] R. A. Briceno, Z. Davoudi and T. C. Luu, Phys. Rev. D **88**, 034502 (2013), arXiv:1305.4903 [hep-lat] (2013).

[42] R. A. Briceno, Z. Davoudi, T. Luu and M. J. Savage, arXiv:1309.3556 [hep-lat] (2013).

[43] W. Detmold and M. J. Savage, Phys. Rev. D **82**, 014511 (2010), arXiv:1001.2768 [hep-lat] (2010).

[44] T. Doi and M. G. Endres, Comput. Phys. Commun. **184**, 117 (2013), arXiv: 1205.0585 [hep-lat] (2012).

[45] S. R. Beane, E. Chang, S. D. Cohen, W. Detmold, H.-W. Lin, T. C. Luu, K. Orginos, A. Parreno, M. J. Savage and A. Walker-Loud, Phys. Rev. Lett. **109**, 172001 (2012), arXiv:1204.3606 [hep-lat] (2012).

[46] N. Barnea, *Nuclear physics with heavy pions — EFT for LQCD*, a talk presented at the *Institute for Nuclear Theory*, July 31, 2013.

[47] J. C. Osborn, R. Babich, J. Brannick, R. C. Brower, M. A. Clark, S. D. Cohen and C. Rebbi, PoS LATTICE 2010, 037 (2010), arXiv:1011.2775 [hep-lat] (2010).

[48] B. Joo, *Computational Challenges in Cold QCD*, a talk at the *Computational Nucl. Phys. Meeting*, Washington, D.C., July 23–24, 2012.

[49] M. T. Hansen and S. R. Sharpe, Phys. Rev. D **86**, 016007 (2012), arXiv:1204.0826 [hep-lat] (2012).

[50] R. A. Briceno and Z. Davoudi, Phys. Rev. D **87**, 094507 (2013), arXiv:1212.3398 [hep-lat] (2012).

[51] P. Guo, J. Dudek, R. Edwards and A. P. Szczepaniak, Phys. Rev. D **88**, 014501 (2013), arXiv:1211.0929 [hep-lat] (2012).

[52] R. A. Briceno and Z. Davoudi, arXiv:1204.1110 [hep-lat] (2012).

[53] K. Polejaeva and A. Rusetsky, Eur. Phys. J. A **48**, 67 (2012), arXiv:1203.1241 [hep-lat] (2012).